

Article

# Static and Fatigue Characterization of Large Composite T-Bolt Connections in Marine Hygrothermal Environments

Paul Murdy <sup>1,\*</sup> , Scott Hughes <sup>1</sup>, David A. Miller <sup>2</sup>, Francisco J. Presuel-Moreno <sup>3</sup> , George T. Bonheyo <sup>4</sup>, Budi Gunawan <sup>5</sup> and Bernadette A. Hernandez-Sanchez <sup>5</sup>

<sup>1</sup> National Renewable Energy Laboratory, 19001 W. 119th Ave., Arvada, CO 80007, USA; scott.hughes@nrel.gov

<sup>2</sup> Mechanical and Industrial Engineering Department, Montana State University, Bozeman, MT 59717, USA; davidmiller@montana.edu

<sup>3</sup> Department of Ocean and Mechanical Engineering, Florida Atlantic University, Boca Raton, FL 33431, USA; fpresuel@fau.edu

<sup>4</sup> Pacific Northwest National Laboratory, 902 Battelle Blvd., Richland, WA 99354, USA; george.bonheyo@pnnl.gov

<sup>5</sup> Advanced Materials Laboratory, Sandia National Laboratories, 1001 University Blvd., Albuquerque, NM 87106, USA; bgunawa@sandia.gov (B.G.); baherna@sandia.gov (B.A.H.-S.)

\* Correspondence: paul.murdy@nrel.gov

**Abstract:** Fiber-reinforced polymer composites have been highlighted as ideal candidates for structural applications in marine renewable energy devices, such as tidal turbines and wave energy converters. It is well understood that harsh marine environments can cause strength degradation of composite laminates, which has been extensively researched at the coupon scale; however, no research has investigated how this translates into larger-scale composite structures. This paper presents a subcomponent-scale study which investigates the effects of hygrothermal aging and subsequent static and fatigue characterization of thick composite T-bolt connections as part of a large, multilaboratory materials research effort. Of the glass-reinforced epoxy and vinylester-epoxy matrix composites tested, both showed measurable static strength degradation (4–36%) after being hygrothermally aged, even though the composite specimens were only partially saturated with water. Under tension–tension fatigue loading, the epoxy specimens performed very well in their dry states but exhibited significant degradation after hygrothermal aging. In comparison, the vinylester-epoxy specimens had much shorter fatigue lives in their dry states but exhibited no degradation after hygrothermal aging. Overall, this research demonstrates that hygrothermal aging can have significant effects on the ultimate strengths and fatigue lives of even partially saturated thick composite T-bolt connections, indicating that degradation of the outer plies on thick composite laminates can have pronounced effects on the whole structure. It discusses the challenges of building an understanding of the effects of harsh marine environments in large-scale composite structures.

**Keywords:** marine renewable energy; composite materials; environmental degradation; hygrothermal aging; bolted connections; structural validation



**Citation:** Murdy, P.; Hughes, S.; Miller, D.A.; Presuel-Moreno, F.J.; Bonheyo, G.T.; Gunawan, B.; Hernandez-Sanchez, B.A. Static and Fatigue Characterization of Large Composite T-Bolt Connections in Marine Hygrothermal Environments. *J. Mar. Sci. Eng.* **2023**, *11*, 2309. <https://doi.org/10.3390/jmse11122309>

Academic Editor: Seyed R. Koloor

Received: 8 November 2023

Revised: 1 December 2023

Accepted: 4 December 2023

Published: 6 December 2023



**Copyright:** © 2023 by the authors. Licensee MDPI, Basel, Switzerland. This article is an open access article distributed under the terms and conditions of the Creative Commons Attribution (CC BY) license (<https://creativecommons.org/licenses/by/4.0/>).

## 1. Introduction

Marine energy resources, such as waves and tidal currents, hold a lot of potential for reliable, clean renewable energy. It is estimated that marine renewable energy (MRE) could account for a significant portion of the United States' utility power generation [1,2]. However, the MRE industry is still fairly nascent. Developing machines to operate reliably for extended periods (decades) in harsh marine environments while also minimizing costs is a difficult challenge and requires well-informed material selection. Composite materials, or fiber-reinforced polymers (FRPs), are regularly highlighted as a suitable option for large, dynamically loaded structures in MRE systems [3]. However, very specific knowledge and expertise are required to design FRP structures effectively. Therefore, the U.S. Department

of Energy's Water Power Technologies Office is currently funding the Marine Energy Advanced Materials project, operated by national laboratories and universities to address knowledge gaps and expedite the adoption of FRPs for MRE structures. Industry surveys were conducted, highlighting the need for better understanding of thick FRP components, bolted connections, and fatigue loading when subjected to harsh marine environments [4].

It is well known that FRPs suffer from varying degrees of degradation when subjected to marine environments [5–9]. Degradation is initiated through water diffusion into the polymeric matrix materials, which is analogous to heat diffusion, and typically presents itself as static and fatigue strength degradation. Water diffusion into composite laminates is a transient process, so outer plies are degraded first, and inner plies follow as the water penetrates deeper into polymer matrices until the laminate becomes fully saturated with water. These diffusion mechanisms and resulting strength degradation are well understood [10–13], but extensive mechanical characterization at the coupon scale is required to properly design large FRP structures for marine environments. However, most coupon-scale studies mainly focus on comparing only dry and fully saturated laminates [9], with little focus on partially saturated laminates. Also, little to no research has been performed to understand how coupon-scale degradation data translate into larger-scale structures with thick FRP laminates [3,14].

Adhesives and/or fasteners are commonly required to connect large FRP components to other components made from dissimilar materials [15]. From an assembly and maintenance standpoint, impermanent fasteners are preferred, such as wind turbine blade root connections [16,17]. T-bolts are commonly used for such root/hub connections (see Figure 1) and are considered a reliable and proven option for attaching thick FRP components to other dissimilar materials [18–20]. Unfortunately, very little research with regards to composite T-bolt connections lies in the public domain and many of the design and failure aspects are closely guarded industry secrets. However, it is anticipated that T-bolt connections could be widely utilized for a variety of MRE system archetypes and therefore the fundamentals should be explored in detail for their use in marine environments.

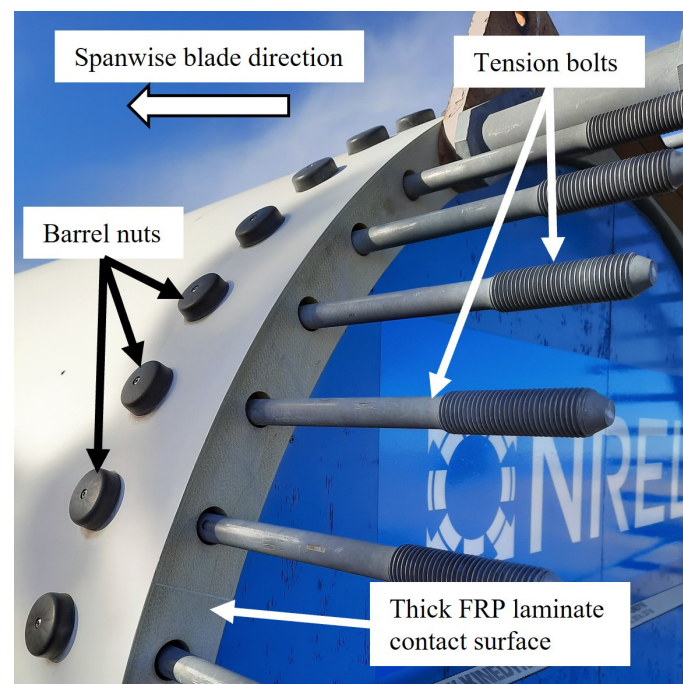


**Figure 1.** An example of T-bolt connections used at a wind turbine blade root with the components labeled.

Based on previous research, similar industry knowledge, and the identified knowledge gaps from the aforementioned industry surveys, a subscale component (or subcomponent) validation effort was developed to address the next level in the commonly used testing

pyramid (see Figure 2), as part of the Marine Energy Advanced Materials project [21]. The resulting study was perhaps the largest of its kind to date, both geographically and with regard to specimen scale. Several specimen geometries were developed, but this paper will only focus on the T-bolt specimens because the testing conducted was the most comprehensive. T-bolt specimens were manufactured by Montana State University (MSU) and the National Renewable Energy Laboratory (NREL) and were then subjected to marine environmental conditions at both Pacific Northwest National Laboratory (PNNL) and Florida Atlantic University (FAU) for extended periods of time. The specimens were then structurally validated at NREL. This paper presents the key findings of this research with the main goals of informing the development and design of FRP components and improving the understanding of design allowables for T-bolt connections when subjected to harsh marine environments. The research takes a novel approach to hygrothermal aging of composite laminates at a scale that has not been explored previously. Ultimately, the developed test methods and final results provide critical guidance on and understanding of the effects of hygrothermal aging on composite laminates at larger scales to marine energy developers.

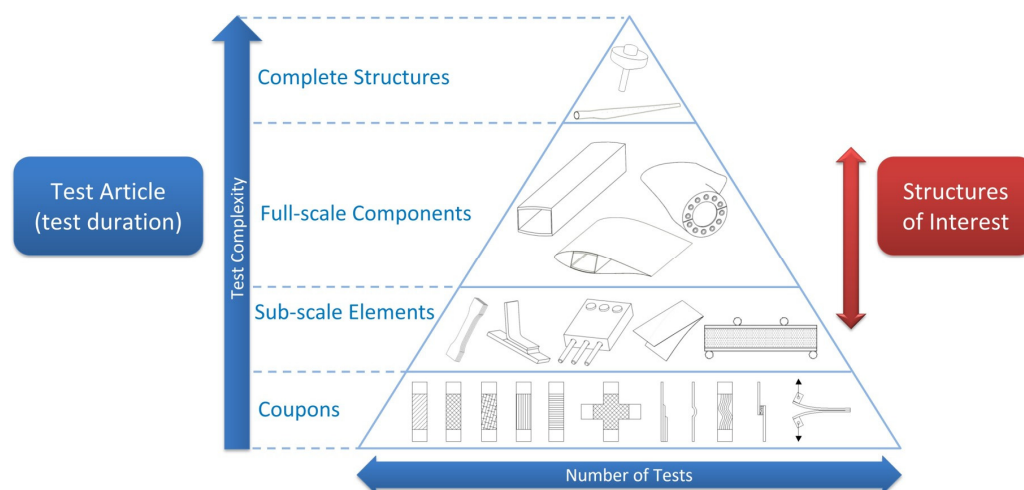


**Figure 2.** The commonly used structural validation pyramid when applied to MRE.

## 2. Experimental Setup

### 2.1. Specimen Design, Materials, and Manufacturing

Large FRP panels were manufactured at MSU by vacuum-assisted resin infusion following ASTM D5687-95 Standard Guide for Preparation of Flat Composite Panels with Processing Guidelines for Specimen Preparation [22]. Heavy-weight quadraxial E-glass fabric (Vectorply E-QX 9000, Phenix City, AL, USA) for the fiber reinforcement and two different resin systems were investigated for matrix materials: a Hexion Epikote MGS RIMR 035c two-part epoxy system (Hexion, Columbus, OH, USA) and a Derakane 411C-350 vinylester-epoxy (VE) system (Ashland Performance Materials, Columbus, OH, USA). Both resin systems are advertised as having good corrosion resistance and have been highlighted as good candidates for the manufacturing of marine energy structures [23]. The resulting glass-reinforced epoxy and VE panels were approximately 43 mm thick.

Double-ended T-bolt specimens were intended to be characterized in a 500 kN load frame, with a focus on testing the composite portions of the specimens to failure and minimizing the probability of fastener failures. The final specimen dimensions were determined through review of previous T-bolt characterization studies [19,20], limited finite element analysis (see Figure 3) (Ansys Workbench 18.0), and relative dimensions from ASTM D5961-17 Standard Test Method for Bearing Response of Polymer Matrix Composite Laminates [24]. The specimens were designed to use 36 mm diameter barrel nuts and M20 tension-bolts. The final specimens were manufactured from the thick composite panels using a combination of waterjet cutting and CNC machining to ensure good dimensional

tolerances for repeatability and alignment during mechanical characterization. This resulted in 26 specimens total—13 with the Hexion epoxy resin system and 13 with the Derakane VE resin system.

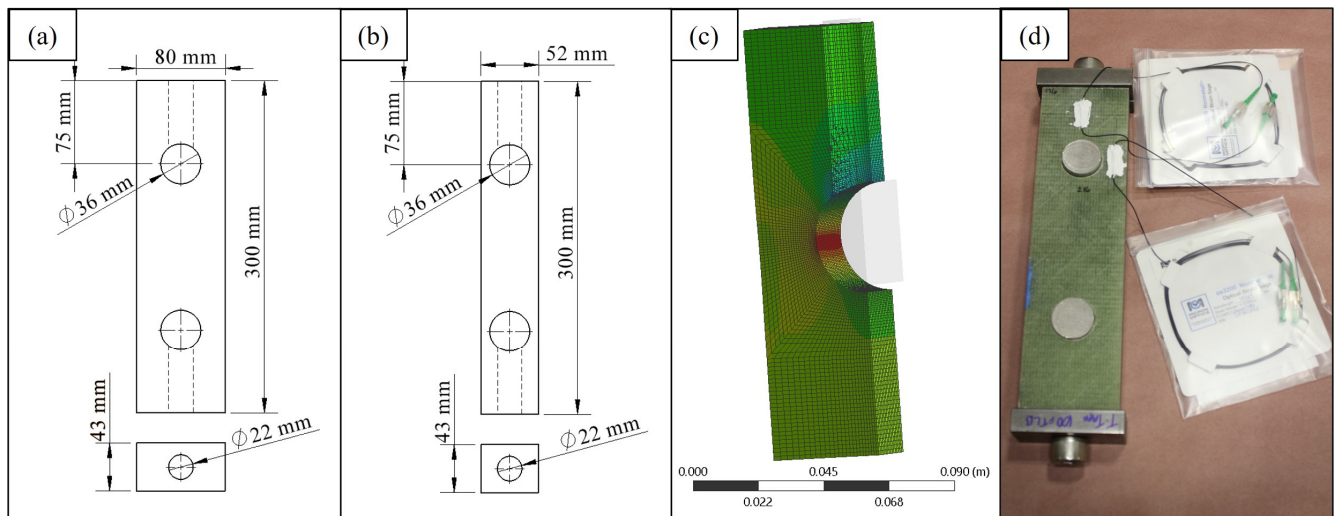


**Figure 3.** (a) Engineering drawings of the T-bolt specimens used for static testing (dimensions in millimeters), (b) engineering drawings of the T-bolt specimens used for fatigue testing (dimensions in millimeters), (c) a finite element model of the as-designed specimen geometry to estimate failure loads, (d) an assembled T-bolt specimen ready for conditioning.

## 2.2. Marine Environmental Conditioning

Prior to environmental conditioning, the specimens were assembled with compression plates and T-bolt hardware to apply preloads to the fasteners and replicate real-life conditions (see Figure 3). Some specimens had Fiber Bragg Grating (FBG) sensors (Luna Innovations, Atlanta, GA, USA) bonded to them to monitor changes in strain through the conditioning periods. Specimen conditioning used ASTM D5229-14 Standard Test Method for Moisture Absorption Properties and Equilibrium Conditioning of Polymer Matrix Composite Materials [25] as guidance. Nine specimens (five epoxy and four VE) were conditioned at FAU at an elevated seawater temperature of 58 °C to accelerate the water absorption process. The tanks were insulated, and salinity was maintained by replacing Atlantic Ocean water every week (see Figure 4). These specimens were conditioned for a total of 380 days. Ten specimens (five epoxy and five VE) were conditioned at PNNL's Marine Sciences Laboratory, where Pacific Ocean water is circulated through the tanks regularly, which also allows for biological growth (see Figure 4). Average temperatures in the tanks are estimated to be around 12 °C but fluctuate throughout the year. Specimens were conditioned there for a total of 527 days. All of the composite specimens were weighed before and after the conditioning periods to evaluate the extent of water absorption that had occurred during the conditioning periods. Specimens were then returned to NREL to be held in cold water storage tanks to maintain their wet conditions while awaiting structural validation. Eight specimens (four epoxy and four VE) remained at NREL and were kept as dry control specimens.

In tandem with the conditioning of the large subcomponents, offcuts from the large panels were used as witness coupons to determine temperature-dependent Fickian diffusion coefficients for the water absorption properties of the “as-manufactured” materials. Flat, thin specimens were conditioned in containers filled with distilled water at both 30 °C and 60 °C according to ASTM D5229-14 [25] for determining moisture absorption properties. Although different from the chemical makeup of the water used for conditioning the T-bolt specimens, distilled water was chosen because salts in the ocean water can significantly interfere with mass measurements, especially when water circulation is minimal. The diffusion coefficients ( $D$ ) were calculated using Equation (1), where  $h$  is the

specimen thickness,  $m_\infty$  is the maximum mass change, and  $k$  is the rate of change of water uptake with regard to the square root of time for the linear portion of the mass uptake slope [26].

$$D = \frac{\pi h^2 k^2}{16 m_\infty^2} \quad (1)$$

The temperature-diffusivity dependence of the materials can then be determined using the Arrhenius relationship (Equation (2)) [26], where  $D_T$  is the diffusion coefficient at any desired temperature ( $T$ ) in Kelvin (K),  $D_0$  is the initial diffusivity, and  $C$  is the activation energy for a given material.

$$D_T = D_0 e^{\frac{-C}{T}} \quad (2)$$

$C$  is determined using Equation (3), the known temperatures ( $T_1$  and  $T_2$ ), and the known Fickian diffusion coefficients ( $D_1$  and  $D_2$ ).

$$C = \frac{\ln\left(\frac{D_1}{D_2}\right)}{\left(\frac{1}{T_2} - \frac{1}{T_1}\right)} \quad (3)$$

$D_0$  can then be determined using Equation (4):

$$D_0 = \frac{D_1}{e^{\frac{-C}{T_1}}} \quad (4)$$

Finally, an acceleration factor ( $A$ ) for equivalent conditioning times at ambient temperatures can be determined using Equation (5) and the calculated water diffusion coefficients at the elevated temperature ( $D_{elev}$ ) and at ambient temperatures ( $D_{amb}$ ).

$$A = \frac{D_{elev}}{D_{amb}} \quad (5)$$

Readers should note that many polymeric materials do not exhibit perfect Fickian diffusion and Arrhenius relationships [27]. This information is being used mainly to estimate conditioning time periods and draw comparisons between the specimens conditioned at ambient temperatures and those exposed to elevated temperatures to accelerate the aging process. This will be explained in detail in Section 3.1.

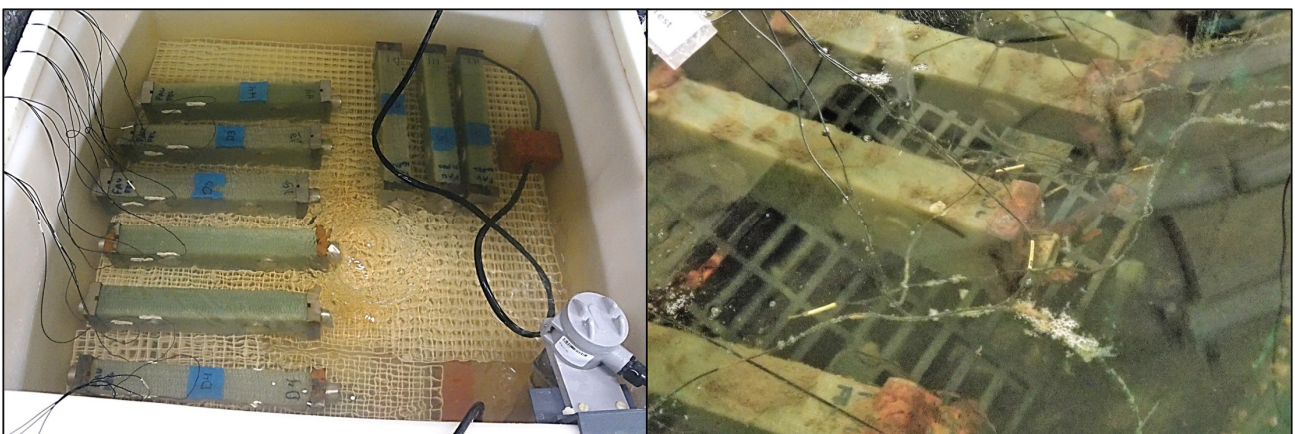


**Figure 4.** (left) Specimens in tanks at elevated temperatures at FAU and (right) specimens in tanks at ambient conditions at PNNL.

### 2.3. Mechanical Characterization

Specimens were characterized under both static and fatigue loading conditions in a 500 kN servo-hydraulic load frame with bespoke fixturing for mounting them (see

Figure 5). AerMet 100 superalloy (Carpenter Technology Corporation, Philadelphia, PA, USA) threaded fasteners and 4340 steel barrel nuts (McMaster-Carr, Elmhurst, IL, USA) were used to mount the composite specimens in the load frame.

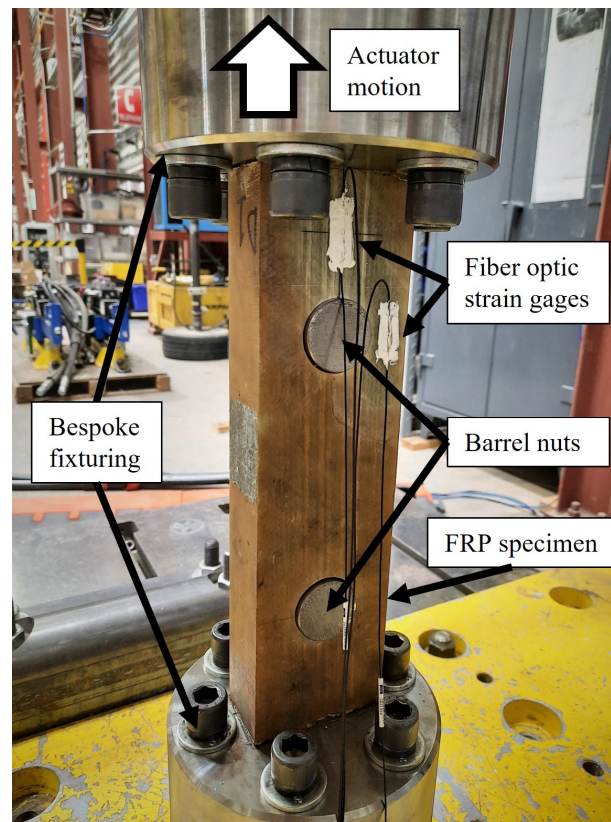


**Figure 5.** A T-bolt specimen in the 500 kN load frame for static testing.

For static testing, the fasteners were torqued to 490 N·m with thread lubricant, which was based on the 75% of the maximum allowable proof stress of the AerMet 100 superalloy. Specimens were pulled to failure in tension at a crosshead speed of  $2 \text{ mm} \cdot \text{min}^{-1}$  to ensure ultimate failure in less than 10 min. Loading rates were determined using ASTM D3039-14 Standard Test Method for Tensile Properties of Polymer Matrix Composite Materials [28]. A total of eleven specimens were characterized under static loading conditions—four dry control specimens, three conditioned at FAU, and four conditioned at PNNL. Many of the specimens were instrumented with resistance-based and FBG strain sensors above and to the side of the specimen through-holes. Occasionally, strain gages were placed on opposing faces of the specimens to verify good load frame alignment with minimal out-of-plane forces being applied. Bearing stresses ( $\sigma_B$ ) and tensile stresses ( $\sigma_T$ ) at the through-hole were calculated using Equations (6) and (7), where  $F$  is the applied force,  $d_{TH}$  is the diameter of the through-hole,  $h$  is the thickness of the specimen,  $d_T$  is the diameter of the tension stud hole, and  $w$  is the width of the specimen.

$$\sigma_B = \frac{F}{d_{TH}h} - \frac{\pi d_T^2}{4} \quad (6)$$

$$\sigma_T = \frac{F}{(w - d_{TH})h} \quad (7)$$

Fatigue testing was performed using ASTM D3479-19 Standard Test Method for Tension-Tension Fatigue of Polymer Matrix Composite Materials [29] as guidance for stress levels and loading rates. Due to limitations of the metallic hardware, the fatigue

specimens had to be modified by reducing their width to encourage failure of the composite laminates. Widths were reduced to 52 mm after environmental conditioning (see Figure 3). Because of this, static and fatigue data are not directly compared in this paper. A total of fourteen specimens were characterized under fatigue loading conditions—four dry control specimens, five conditioned at FAU, and five conditioned at PNNL. Due to the limited number of specimens of the various materials and conditioning locations, the goal of the fatigue testing was to apply the same fatigue stress levels to all specimens and encourage fatigue failures in the range of  $10^5$  to  $10^6$  cycles. Through preliminary tests, this was determined to be  $\sigma_T = 130$  MPa. All specimens were tested under tension–tension loading where  $\frac{\sigma_{T,min}}{\sigma_{T,msc}} = 0.1$ . Similar strain gage instrumentation was utilized to track stiffness degradation trends, and thermocouples were used to monitor specimen surface temperatures and ensure that they did not exceed 5 °C above ambient due to applied strain rates. The T-bolt fasteners for every specimen were torqued to 305 N·m to prevent separation (or lash) between the specimens and the load fixture.

### 3. Results and Discussion

#### 3.1. Water Absorption

After the conditioning periods were complete, specimens were returned to NREL wrapped in cellophane to minimize water desorbing from the composites. Their hardware was disassembled, and the surfaces of the composites were cleaned of any corrosion and biological growth. Specimens were then dried of surface water and weighed. Table 1 shows the resulting percentage changes in specimen mass and standard deviations as an indication of total water absorption into the composite matrices during the conditioning periods.

**Table 1.** Percentage mass change of the T-bolt specimens after their conditioning periods at FAU and PNNL.

Matrix Material	Conditioning Location	Mass Change (%)
Epoxy	PNNL	0.58 ± 0.27
	FAU	1.12 ± 0.03
Vinylester-epoxy	PNNL	0.60 ± 0.24
	FAU	0.54 ± 0.04

The epoxy specimens conditioned at FAU gained significantly more mass than any of the other specimens, especially the VE specimens under the same conditions. Both the epoxy and VE specimens conditioned at PNNL exhibited comparable average mass changes, although variability between specimens was much higher. Corrosion from that hardware was much more extensive on the surfaces of those specimens and was difficult to fully remove before weighing. Some biological growth was also difficult to remove. The combination of these two aspects is a likely cause for the increased variability, and they potentially artificially increased the perceived total amount of water absorption. Because of this, it appears that the VE specimens absorbed comparable amounts of water at FAU and PNNL. The changes in mass of the specimens hygrothermally aged at FAU were much more consistent.

Inspection of the data collected during coupon-scale water absorption studies sheds some light on the differences observed for the subcomponent-scale T-bolt specimens. Table 2 presents a summary of the water absorption variables obtained during the coupon-scale testing and those calculated using Equations (1)–(5). Figure 6 also shows a plot of calculated temperature-dependent diffusion coefficients for both the epoxy and VE composites.

The first key comparison between the T-bolt data set and the coupon-scale diffusion data are the  $m_\infty$  values, particularly for the VE composites. The changes in mass of the VE T-bolt specimens hygrothermally aged at PNNL were close to and in some cases exceeded the  $m_\infty$  values observed at the coupon scale. This is a clear indication that the observed surface contamination and biological growth on the T-bolt specimens from

PNNL artificially inflated the results shown in Table 1. This may also be the case for the specimens conditioned at FAU but to a much lesser extent. It was expected that the T-bolt specimens would not reach full saturation within the time constraints of this study, due to the laminate thickness.

**Table 2.** Comparison of temperature-dependent Fickian water absorption parameters obtained from coupon-scale testing of the epoxy and VE composites. Parameters below the dividing line indicate temperature-dependent diffusion parameters calculated using the coupon-scale test data and Arrhenius relationships and the assumed diffusion coefficients for the T-bolt conditioning temperatures at FAU and PNNL.

	Epoxy	Vinylester-Epoxy
$m_{\infty}$ (%)	1.44	0.66
$D_{30}$ ( $m^2 \cdot s^{-1}$ )	$1.02 \times 10^{-13}$	$4.49 \times 10^{-13}$
$D_{60}$ ( $m^2 \cdot s^{-1}$ )	$1.94 \times 10^{-12}$	$1.36 \times 10^{-12}$
C (K)	9912.9	3737.9
$D_0$ ( $m^2 \cdot s^{-1}$ )	16.27	$1.02 \times 10^{-7}$
$D_{FAU}$ ( $m^2 \cdot s^{-1}$ )	$1.60 \times 10^{-12}$	$1.27 \times 10^{-12}$
$D_{PNNL}$ ( $m^2 \cdot s^{-1}$ )	$1.28 \times 10^{-14}$	$2.05 \times 10^{-13}$
A	125.0	6.20
Equivalent time of FAU specimens at PNNL (years)	130.0	6.45

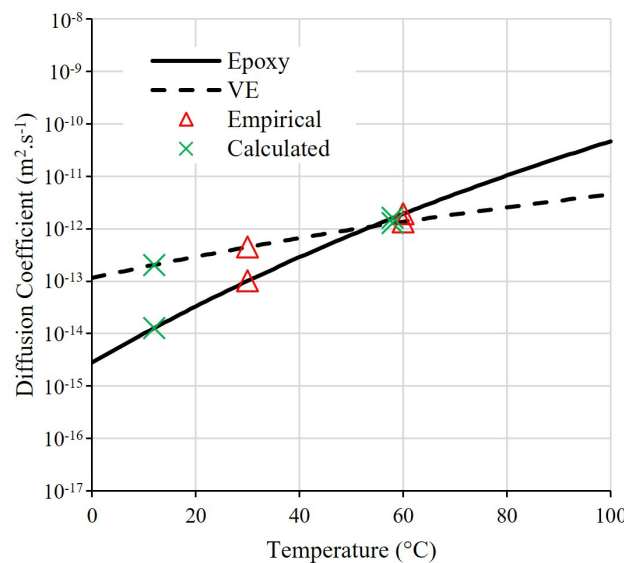


**Figure 6.** Plot showing calculated temperature-dependent water diffusion coefficients for the epoxy and VE composites used in this study.

Another interesting observation was the temperature dependence of the diffusion coefficients. Changes in conditioning temperature appear to have a much more pronounced effect on diffusion coefficients for the epoxy composites compared to the VE composites. This is also reflected when comparing acceleration factors for those specimens conditioned at FAU. The acceleration factor for the epoxy composite was calculated to be more than 20 times greater than that of the VE composite. Therefore, the equivalent conditioning time of the epoxy specimens conditioned in 58 °C water at FAU was calculated to be 130 years in 12 °C water at PNNL. Obviously, 130 years would far exceed the necessary usable life of any renewable energy structure, which is typically 20–30 years. In comparison, the same acceleration factor calculation yields an estimated 6.45-year conditioning period for the VE T-bolt specimens under PNNL’s ambient conditions. This is a much more realistic time frame for any composite structure currently being deployed as part of an MRE system.

Ultimately, this highlights fundamental differences between FRP matrices when conducting artificial aging studies at larger scales for marine applications, particularly when deployment time frames are known. The data presented here should help guide conditioning periods for future studies at subcomponent and component scales and should help with incorporating composite structures into high-risk MRE deployments. Again, readers should note that the equivalent conditioning time data have been presented as estimates and as a means for making comparisons between the T-bolt specimens conditioned at FAU and PNNL with regard to mass changes and the mechanical strength data presented in the proceeding sections. It is based on the assumptions that both the epoxy and VE composites follow ideal Fickian diffusion and Arrhenius relationships, which are unaffected by the different water chemistries used in this study. This may not be the case for many polymeric composite materials. It also negates any anisotropic differences in diffusion coefficients, which is often the case with FRPs.

### 3.2. Static Strength Characterization

Table 3 shows ultimate bearing strength comparisons of all the T-bolt specimens characterized through static loading conditions. All final failure modes were observed as bearing failures at the barrel nuts (see Figure 7), which also resulted in lengthwise delaminations around the tension bolt hole. Overall, the results show that the VE specimens performed better than their epoxy counterparts under static loading conditions.

**Table 3.** Static bearing strength results for all the specimens tested under static loading conditions. Note that only one vinylester-epoxy specimen was tested under dry conditions.

Matrix Material	Conditioning Location	Bearing Strength (MPa)	Percent Degradation (%)
Epoxy	Dry	265.1 ± 5.6	-
	PNNL	255.3 ± 26.4	3.7
	FAU	171.1 ± 21.8	35.5
Vinylester-epoxy	Dry	311.9 ± 0.0	-
	PNNL	290.1 ± 2.4	7.0
	FAU	242.0 ± 21.7	22.4

With regard to the specimens hygrothermally aged at FAU, strength degradation was observed due to the environmental aging process. Negligible changes in bearing strength were determined for the specimens hygrothermally aged at PNNL, especially when considering the limited number of specimens that were available to test under each condition. The specimens hygrothermally aged under accelerated conditions at FAU exhibited larger degradations in strength. On average, the epoxy specimens suffered a 36% reduction in ultimate bearing strength compared to a 22% reduction for the VE specimens. This is no surprise when comparing the differences in temperature-dependent water diffusion coefficients and the significant differences in equivalent conditioning times for the two materials. Nonetheless, it should be acknowledged that these results indicate that marine environmental aging and associated water absorption mechanisms on thick FRPs can have pronounced effects on the mechanical strength of T-bolt connections that should be accounted for in the MRE structural design process.

Figure 8 shows comparisons of tensile strains measured on the T-bolt FRP laminates to the side of the barrel nuts when compared with  $\sigma_B$ . Generally, it appears that the environmental aging process had little effect on the stiffness of the specimens, as is consistent with previous research [23]. Degradation in water primarily influences the polymer matrix and fiber/matrix interface, so does not typically influence stiffness in fiber-dominant laminates, like the T-bolt specimens in this study. Variations in the slope of the stress-strain curves may be attributed to slight differences in alignment of the specimens in the load frame during testing.

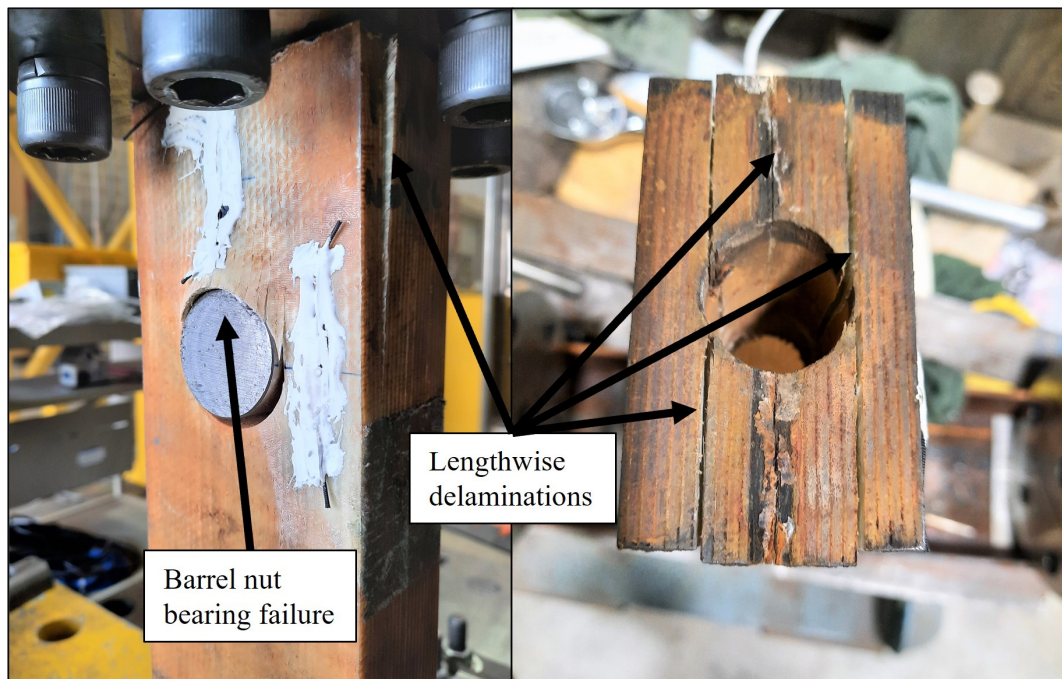


**Figure 7.** Photos of typical ultimate bearing failures at the through-holes observed during static testing and resulting lengthwise delaminations around the tension holes.

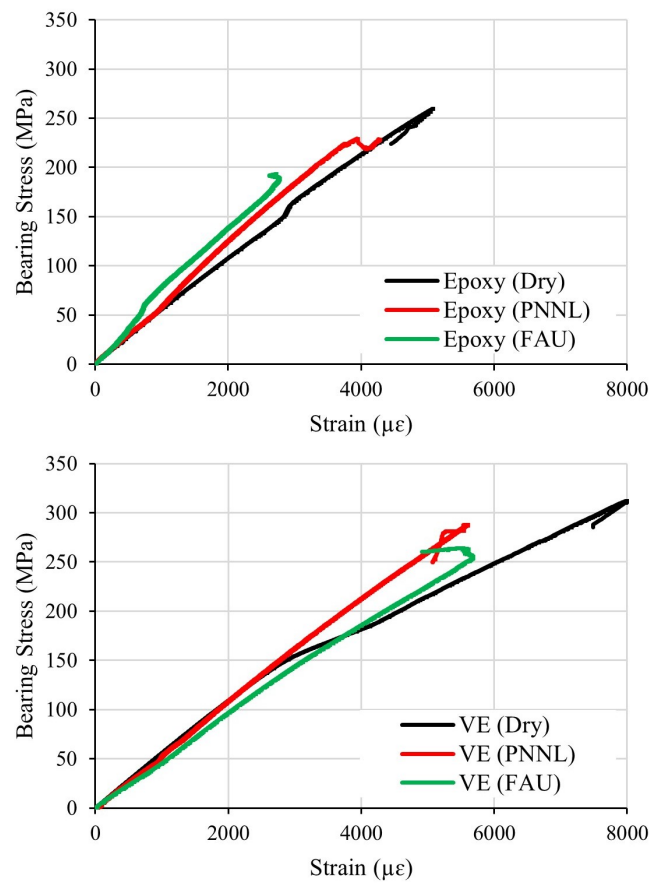


**Figure 8.** Comparisons of bearing stresses against measured tensile strains on the composite surfaces to the side of the barrel nuts on the epoxy and VE T-bolt specimens.

### 3.3. Fatigue Strength Characterization

Due to limitations of the T-bolt hardware, the fatigue specimens were modified to ensure failure of the FRP laminate by reducing their widths. Because of this, the fatigue data cannot be compared directly with the static test data. Also, specimen modifications were performed after the specimens had been hygrothermally aged, so the water absorption boundary conditions were also modified—two faces that were exposed to water were removed. One perspective is that it may be a more representative boundary condition for larger-scale structures, which would be made up of an array of T-bolt connections with no side faces that are exposed to water.

Figure 9 shows the average cycles-to-failure for the reduced-width T-bolt specimens tested in fatigue, plotted on a logarithmic scale to properly visualize the significant differences observed between the data sets. All specimens exhibited tensile failures at the side of the barrel nuts (see Figure 10). Comparisons between the materials and hygrothermal aging conditions showed some significant differences. The dry epoxy specimens had significantly better fatigue lives than their VE counterparts for the prescribed loading. On average, their cycles-to-failure were almost 100 times greater than the VE composite specimens. However, the VE specimens exhibited little to no degradation in cycles-to-failure due to the conditioning at PNNL and FAU. The number of specimens available was insufficient to observe statistically significant differences. Previous coupon-scale research on glass-fiber-reinforced vinylester and epoxy laminates for wind turbine blades by Mandell et al. [30] showed that VE laminates typically have comparable static ultimate strengths to equivalent epoxy matrix composites; however, their fatigue strengths appeared to be much more susceptible to laminate complexity, such as off-axis stress states and fiber waviness. This was observed as steeper fatigue curves when comparing stress levels with cycles-to-failure.

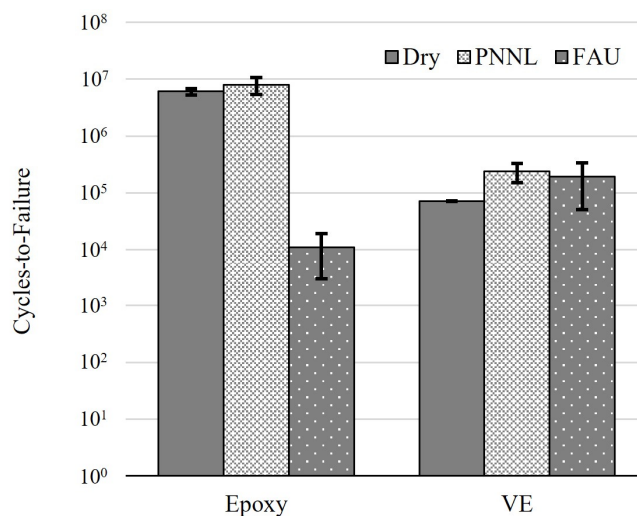


**Figure 9.** Bar chart of cycles-to-failure for all specimens tested under tension–tension fatigue loading conditions ( $\sigma_T = 130$  MPa) after being subjected to the various marine environments (error bars represent standard deviations).

With regard to the hygrothermally aged epoxy specimens, no statistically significant degradation was observed for the specimens aged at PNNL. These specimens were conditioned at ambient temperature. Therefore, the 527 days they spent conditioning was the equivalent of 570 days, unlike the specimens conditioned at FAU, which had much longer equivalent conditioning times due to their elevated temperatures. The water diffusion process is very slow at lower temperatures, so it is unlikely that the water had penetrated very deep into the laminates and caused a statistically significant amount of degradation. The specimens conditioned at FAU exhibited severe degradation when exposed to fatigue loading—on average, an almost three orders of magnitude reduction in cycles-to-failure. This is not surprising given the acceleration factor calculated in Section 3.1 for the epoxy

matrix material exposed to the elevated water temperatures. However, these results do imply that even partially saturated thick FRP laminates are susceptible to severe fatigue strength degradation when exposed to the right environmental conditions.



**Figure 10.** A typical through-hole tensile failure of the T-bolt fatigue specimens.

Figure 11 shows a comparison of tensile stiffness trends over the fatigue lives of specimens exposed to the various hygrothermal environments. In this case, peak–valley actuator displacement is used as a means of comparing stiffness changes for the duration of the fatigue tests. Generally, the specimens followed typical FRP composite fatigue life trends, whereby the majority of the stiffness degradation occurred during the initial and last 10% of the specimens' fatigue lives [31]. Variations in stiffness between specimens are mainly attributed to variabilities in the pretension applied to the tension bolts when tightening them to known torques during the installation of the specimens in the test fixture. These variations were realized during preliminary fatigue testing (prior to reducing the width of the fatigue specimens). Force displacement plots show steeper trends with increased bolt tension. Although bolt tension should not affect the stiffness of a flat, regular-bolted joint, this may not be true for the T-bolt configuration, which applies a more complex stress state to the composite laminate. Torque wrenches and thread lubricant were used to apply tension to the studs, which can inherently cause up to  $\pm 10\%$  variability in applied tension.

Final considerations when comparing the presented fatigue data are (1) the differences in time that specimens spent in the cold water tanks “maintaining” their partially saturated conditions while awaiting fatigue testing and (2) the amount of time spent out of water during the fatigue testing. The fatigue testing portion of this study took significantly longer than the static testing portion. With specimen fatigue lives in the range of  $10^4$  to  $10^7$  cycles-to-failure, testing times ranged from a matter of hours to up to 30 days of continuous

run time. Therefore, the final specimens to be tested had been held in the cold water tanks for significantly longer than those that were tested first. Rather than test the specimens in batches (i.e., all the VE specimens from PNNL, then all the epoxy specimens from FAU), specimens were tested in a randomized order. This was done in an attempt to negate potential effects on fatigue results caused by some specimens spending more time than others in cold water tanks awaiting testing; however, this detail cannot be ignored when making comparisons. The level of project planning required to mitigate this would not be feasible under most circumstances.

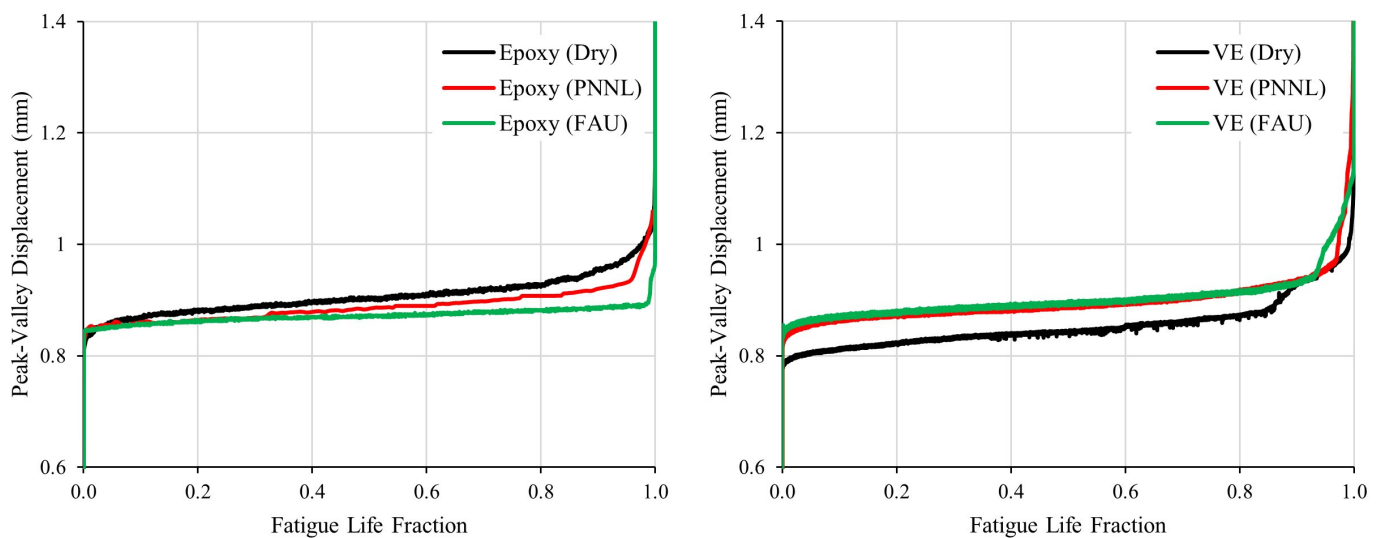


**Figure 11.** A comparison of specimen stiffness (peak–valley actuator displacement) trends against fatigue life fraction for specimens loaded in tension–tension fatigue.

Also, the specimens were fatigue tested with no method of keeping them wet throughout the fatigue test. For specimens with fatigue lives shorter than  $10^5$  cycles, this is unlikely to have significantly influenced the results, but may have had an effect on the longer-duration fatigue tests. Past research has shown that some strength properties of hygrothermally aged FRPs can be recovered by drying the laminates [23]. There is a possibility that specimen fatigue lives for the longer duration tests may have been extended by this phenomenon. However, previous research has also shown that submerging specimens in water when applying fatigue loading can have a pronounced effect on fatigue lives through the capillary action of water into transverse matrix cracks in FRP laminates [32–34]. This drives different damage mechanisms and ultimately different failure modes caused by less realistic edge conditions. Despite these known phenomena, neither immersed fatigue loading nor sequential (hygrothermal aging then fatigue loading) testing approaches perfectly capture realistic environmental and loading effects on the same time scales for accelerated testing. Future research in this domain will be focused on realistically capturing these synergistic effects to better guide MRE industry decisions on more appropriate testing at the subcomponent scale and up.

#### 4. Conclusions

As part of a multilaboratory materials research initiative funded by the U.S. Department of Energy, a landmark hygrothermal aging study on FRP subcomponents was conducted. The primary goals of the project were informing the MRE industry on design allowables of thick bolted connections in marine environments and ultimately reducing barriers and uncertainties to adopting advanced composite materials for MRE structures. This paper has presented a portion of this study aimed at understanding marine environmental effects on T-bolt connections specifically.

The key takeaways were that the marine environment can have pronounced effects on the strength of thick FRP composites, even if only partially saturated, due to the water absorption process. Inspection of temperature-dependent water absorption diffusion coefficients showed that controlling time scales with multiple materials at elevated temperatures is difficult and requires former knowledge from coupon-scale test data as well as detailed project planning. In the future, better understanding of these effects is required to perform representative studies that match intended time frames for renewable energy structures. Static strength testing showed that degradation was measurable even for the specimens subjected to marine environments at ambient temperatures. Similar comparisons could not be made for the fatigue test data due to the limited numbers of specimens and increased statistical variations. However, significant differences were observed between the fatigue strengths of the epoxy and VE matrix composites that were tested, which is valuable information in terms of material selection.

Future research will be focused on two main areas:

1. Constructing realistic numerical finite difference and finite element models to represent the processes of water diffusion into thick FRPs to understand the depth of penetration and to ultimately apply strength degradation criteria to accurately predict the failure of thick FRP structures when subjected to harsh marine environments. This will require extensive orthotropic water diffusion and strength properties of the materials. The models will be validated using the test data from this study;
2. Development of test methods for accurately representing time, temperature, loading, and water absorption effects simultaneously at laboratory scales to truly understand their synergistic effects.

Ultimately, this research hopes to continue to provide valuable knowledge and testing frameworks to the MRE industry for adopting advanced composite materials.

**Author Contributions:** Conceptualization, P.M., S.H., D.A.M., G.T.B. and B.A.H.-S.; methodology, P.M., S.H., D.A.M., F.J.P.-M., G.T.B. and B.G.; validation, P.M.; formal analysis, P.M.; investigation, P.M., S.H. and B.G.; data curation, P.M.; writing—original draft preparation, P.M.; writing—review and editing, P.M., S.H., D.A.M., F.J.P.-M., G.T.B., B.G. and B.A.H.-S.; funding acquisition, S.H., D.A.M., F.J.P.-M., G.T.B. and B.A.H.-S. All authors have read and agreed to the published version of the manuscript.

**Funding:** This work was authored in part by the National Renewable Energy Laboratory, operated by Alliance for Sustainable Energy, LLC, for the U.S. Department of Energy (DOE) under Contract No. DE-AC36-08GO28308. Funding provided by the U.S. Department of Energy Office of Energy Efficiency and Renewable Energy Water Power Technologies Office. The views expressed in the article do not necessarily represent the views of the DOE or the U.S. Government. The U.S. Government retains and the publisher, by accepting the article for publication, acknowledges that the U.S. Government retains a nonexclusive, paid-up, irrevocable, worldwide license to publish or reproduce the published form of this work, or allow others to do so, for U.S. Government purposes.

**Institutional Review Board Statement:** Not applicable.

**Informed Consent Statement:** Not applicable.

**Data Availability Statement:** Data is available by request to the corresponding author, Paul Murdy (paul.murdy@nrel.gov).

**Acknowledgments:** First and foremost, we would like to thank our project leads from the U.S. Department of Energy's Water Power Technologies Office, Lauren Ruedy and Carrie Noonan, for their support, feedback, and guidance throughout the project, as well as the laboratories, researcher, and partners that made considerable contributions to this research project. Also, this project would not have been possible without technician support from Sara Wallen, David Barnes, Victor Castillo, Mike Jenks, and Bill Gage.

**Conflicts of Interest:** The authors declare no conflict of interest.

## References

1. Haas, K.A.; Fritz, H.M.; French, S.P.; Smith, B.T.; Neary, V. *Assessment of Energy Production Potential from Tidal Streams in the United States*; Georgia Institute of Technology: Atlanta, GA, USA, 2011.
2. Jacobson, P.T.; Hagerman, G.; Scott, G. *Mapping and Assessment of the United States Ocean Wave Energy Resource*; Electric Power Research Institute: Palo Alto, CA, USA, 2011.
3. Alam, P.; Robert, C.; Ó Brádaigh, C.M. Tidal turbine blade composites—A review on the effects of hygrothermal aging on the properties of CFRP. *Compos. Part B Eng.* **2018**, *149*, 248–259. [[CrossRef](#)]
4. Hernandez-Sanchez, B.A.; Gunawan, B.; Nicholas, J.; Miller, D.; Bonheyo, G.; Murdy, P.; Hughes, S.; Presuel-Moreno, F. *Developing Materials for Marine Renewable Energy Technologies*; Sandia National Lab.(SNL-NM): Albuquerque, NM, USA, 2019.
5. Nash, N.H.; Portela, A.; Bachour, C.; Manolakis, I.; Comer, A.J. Effect of environmental conditioning on the properties of thermosetting- and thermoplastic-matrix composite materials by resin infusion for marine applications. *Compos. Part B Eng.* **2019**, *177*, 107271. [[CrossRef](#)]
6. Gagani, A.I.; Mialon, E.P.V.; Echtermeyer, A.T. Immersed interlaminar fatigue of glass fiber epoxy composites using the I-beam method. *Int. J. Fatigue* **2019**, *119*, 302–310. [[CrossRef](#)]
7. Davies, P.; Arhant, M. Fatigue Behaviour of Acrylic Matrix Composites: Influence of Seawater. *Appl. Compos. Mater.* **2019**, *26*, 507–518. [[CrossRef](#)]
8. Cavasin, M.; Sangermano, M.; Thomson, B.; Giannis, S. Exposure of Glass Fiber Reinforced Polymer Composites in Seawater and the Effect on Their Physical Performance. *Materials* **2019**, *12*, 807. [[CrossRef](#)]
9. Nunemaker, J.D.; Voth, M.M.; Miller, D.A.; Samborsky, D.D.; Murdy, P.; Cairns, D.S. Effects of moisture absorption on damage progression and strength of unidirectional and cross-ply fiberglass-epoxy laminates. *Wind Energy Sci.* **2018**, *3*, 427–438. [[CrossRef](#)]
10. Heide-Jørgensen, S.; Ibsen, C.H.; Budzik, M.K. Temperature dependence of moisture diffusion in woven epoxy-glass composites: A theoretical and experimental study. *Mater. Today Commun.* **2021**, *29*, 102844. [[CrossRef](#)]
11. Shan, M.; Zhao, L.; Hong, H.; Liu, F.; Zhang, J. A progressive fatigue damage model for composite structures in hygrothermal environments. *Int. J. Fatigue* **2018**, *111*, 299–307. [[CrossRef](#)]
12. Linde, E.; Giron, N.H.; Celina, M.C. Water diffusion with temperature enabling predictions for sorption and transport behavior in thermoset materials. *Polymer* **2018**, *153*, 653–667. [[CrossRef](#)]
13. Korkees, F.; Alston, S.; Arnold, C. Directional diffusion of moisture into unidirectional carbon fiber/epoxy Composites: Experiments and modeling. *Polym. Compos.* **2018**, *39*, E2305–E2315. [[CrossRef](#)]
14. Finnegan, W.; Jiang, Y.; Meier, P.; Hung, L.C.; Fagan, E.; Wallace, F.; Glennon, C.; Flanagan, M.; Flanagan, T.; Goggins, J. Numerical modelling, manufacture and structural testing of a full-scale 1 MW tidal turbine blade. *Ocean Eng.* **2022**, *266*, 112717. [[CrossRef](#)]
15. Camanho, P.P.; Matthews, F.L. Stress analysis and strength prediction of mechanically fastened joints in FRP: A review. *Compos. Part A Appl. Sci. Manuf.* **1997**, *28*, 529–547. [[CrossRef](#)]
16. Lee, H.G.; Kang, M.G.; Park, J. Fatigue failure of a composite wind turbine blade at its root end. *Compos. Struct.* **2015**, *133*, 878–885. [[CrossRef](#)]
17. Bender, J.J.; Hallett, S.R.; Lindgaard, E. Investigation of the effect of wrinkle features on wind turbine blade sub-structure strength. *Compos. Struct.* **2019**, *218*, 39–49. [[CrossRef](#)]
18. Lillo, P.; Crawford, C. Analysis of Embedded Blade Root Carrot and T-Bolt Connections Subject to Cold Weather Conditions Using a Finite Element Model. In Proceedings of the ASME 2010 International Mechanical Engineering Congress and Exposition, Vancouver, BC, Canada, 12–18 November 2010; pp. 1035–1045. [[CrossRef](#)]
19. Ashworth Briggs, A.; Zhang, Z.; Dhakal, H. T-Bolt Bearing Strengths in Composite Blade Applications. In Proceedings of the ECCM15—15th European Conference on Composite Materials, Venice, Italy, 24–28 June 2012.
20. Ashworth Briggs, A.; Zhang, Z.Y.; Dhakal, H. Study on T-bolt and pin-loaded bearing strengths and damage accumulation in E-glass/epoxy blade applications. *J. Compos. Mater.* **2015**, *49*, 1047–1056. [[CrossRef](#)]
21. Murdy, P.; Hughes, S.; Miller, D.; Presuel-Moreno, F.; Bonheyo, G.; Hernandez-Sanchez, B.; Gunawan, B. *Subcomponent Validation of Composite Joints for the Marine Energy Advanced Materials Project*; National Renewable Energy Lab. (NREL): Golden, CO, USA, 2023.
22. D5687/D5687M-95; Standard Guide for Preparation of Flat Composite Panels with Processing Guidelines for Specimen Preparation. ASTM International: West Conshohocken, PA, USA, 2015. [[CrossRef](#)]
23. Miller, D.A.; Samborsky, D.D.; Stoffels, M.T.; Voth, M.M.; Nunemaker, J.D.; Newhouse, K.J.; Hernandez-Sanchez, B.A. *Summary of Marine and Hydrokinetic (MHK) Composites Testing at Montana State University*; Sandia National Lab. (SNL-NM): Albuquerque, NM, USA, 2020.
24. ASTM D5961/D5961M-17; Standard Test Method for Bearing Response of Polymer Matrix Composite Laminates. ASTM International: West Conshohocken, PA, USA, 2017. [[CrossRef](#)]
25. ASTM D5229/D5229M-14; Standard Test Method for Moisture Absorption Properties and Equilibrium Conditioning of Polymer Matrix Composite Materials. ASTM International: West Conshohocken, PA, USA, 2014. [[CrossRef](#)]
26. Shen, C.-H.; Springer, G.S. Moisture Absorption and Desorption of Composite Materials. *J. Compos. Mater.* **1976**, *10*, 2–20. [[CrossRef](#)]
27. Grace, L.R.; Altan, M.C. Characterization of anisotropic moisture absorption in polymeric composites using hindered diffusion model. *Compos. Part A Appl. Sci. Manuf.* **2012**, *43*, 1187–1196. [[CrossRef](#)]

28. ASTM D3039/D3039M-14; Standard Test Method for Tensile Properties of Polymer Matrix Composite Materials. ASTM International: West Conshohocken, PA, USA, 2014. [[CrossRef](#)]
29. ASTM D3479/D3479M-19; Standard Test Method for Tension-Tension Fatigue of Polymer Matrix Composite Materials. ASTM International: West Conshohocken, PA, USA, 2019. [[CrossRef](#)]
30. Mandell, J.F.; Samborsky, D.D.; Miller, D.A.; Agastra, P.; Sears, A.T. *Analysis of SNL/MSU/DOE Fatigue Database Trends for Wind Turbine Blade Materials, 2010–2015*; Sandia National Labs: Albuquerque, NM, USA, 2016.
31. Reifsnider, K. Fatigue behavior of composite materials. *Int. J. Fract.* **1980**, *16*, 563–583. [[CrossRef](#)]
32. Selvarathinam, A.S.; Weitsman, Y.J. Transverse cracking and delamination in cross-ply gr/ep composites under dry, saturated and immersed fatigue. *Int. J. Fract.* **1998**, *91*, 103–116. [[CrossRef](#)]
33. Selvarathinam, A.S.; Weitsman, Y.J. A shear-lag analysis of transverse cracking and delamination in cross-ply carbon-fibre/epoxy composites under dry, saturated and immersed fatigue conditions. *Compos. Sci. Technol.* **1999**, *59*, 2115–2123. [[CrossRef](#)]
34. Siriruk, A.; Penumadu, D. Degradation in fatigue behavior of carbon fiber–vinyl ester based composites due to sea environment. *Compos. Part B Eng.* **2014**, *61*, 94–98. [[CrossRef](#)]

**Disclaimer/Publisher’s Note:** The statements, opinions and data contained in all publications are solely those of the individual author(s) and contributor(s) and not of MDPI and/or the editor(s). MDPI and/or the editor(s) disclaim responsibility for any injury to people or property resulting from any ideas, methods, instructions or products referred to in the content.